Ibn Al-Haitham Journal for Pure and Applied Sciences
Journal homepage: jih.uobaghdad.edu.iq
PISSN: 1609-4042, EISSN: 2521-3407
IHJPAS. 2024, 37(3)

Synthesis and Physical Characterization of Manganese DioxideNanoparticles Using Leek Extract for Antibacterial Application

Rand A. Hayder [1*] and Zainab J. Shanan[2]
[1,2]Department of Physics, College of Sciences for Women, University of Baghdad, Baghdad, Iraq.
*Corresponding Author.

Received:19 May 2023 Accepted:20 June 2023 Published:20 July 2024
doi.org/10.30526/37.3.3503

Abstract
Manganese dioxide nanoparticles were synthesized by the green method using leek with Manganous Sulphate Monohydrate, ($MnSO_4.H_2O$) in an environmentally friendly manner. The obtained MnO_2 particle was characterized by x-ray diffraction (XRD), field scanning electron microscopy (FESEM), atomic force microscopy (AFM), and (UV-Visible) spectroscopy. The X-ray diffraction pattern showed peaks belonging to manganese oxide nanoparticles; 34.07 nm is the average crystalline size. From the field-scanning electron microscopy (FESEM) image, the surface morphology shows that the nanoparticles are spherical and rocky in shape. An atomic force microscopy (AFM) atomic force microscope was used to show MnO_2 NP_s as agglomerated particles with an average diameter of (50.20) nm. The absorption spectrum of MnO_2 nanoparticles was determined using UV-visible, and the energy band was measured to be (4.31) eV. The results show that the band gap energy increases with decreasing particle size. The antibacterial property of nanoparticles was observed. These materials' antibacterial effects were examined utilizing some common Gram-positive and Gram-negative bacteria**.** The synthesis of MnO_2-NP_s inhibited the growth of S. aureus, k. pneumoniae, and E. coli, with half-dilutions. MnO_2-NP_s have shown good inhibition for S. aureus and lower efficient antibacterial activity against the bacterial k. pneumonia and E. coli, and the higher activity was at a concentration of (1000μg/ml).
Keywords: Manganese Dioxide, nanoparticles, green synthesis, antibacterial activity, E.coli.

1. Introduction
Biotechnology and nanotechnology are advancing, and this opens the way for study into the creation of nanoparticles. For the treatment of cancer, allergies, diabetes, inflammation, and infections, nanoparticles are widely used. It has a variety of uses in the fields of biomedical devices, renewable energy, cosmetics, medicine, and cleaning the environment[1, 2]. Due to their high specific surface area and recognized antibacterial activity, magnetic properties, catalytic, and optical characteristics, and metal NP_s have been the subject of substantial research [3,4]. Manganese Dioxide is a well-known example of a nanoparticle that is usually utilized and has distinct optical, thermal, mechanical, chemical, and electrical properties[5, 6]. Because biological components serve as reducing as well as capping agents and do not require high energy, harmful chemicals, high pressures, or other processes, the green synthesis of nanoparticles is an

environmentally benign method [7]. The source of plant extracts determines how nanoparticles can be identified. Plant extracts have stabilizing and reducing effects[8].

Polyphenols, alkaloids, terpenoids, and flavonoids, are just a few of the phytochemical components found in plants that have been proven to cause metal ion reduction and the eventual formation of metal nanoparticles[9]. Additionally, compared to extracts, it is thought that phytomolecules from biogenic plants could improve their inherent capabilities, such as antibacterial, antioxidant, and anticancer[10]. Thus, green synthesis utilizing plant leaf extract improves the biocompatibility of nanoparticles and is the cause of the synergistic impact [11]. NP_s and other nonmaterials are attracting much interest due to their distinctive physical properties. Furthermore, because of their physical properties, NP_s are ideal for use in biological, electrical, sensing, and optoelectronic applications[12].In this research, manganese dioxide nanoparticles are prepared in an environmentally friendly manner. Green synthesis is important as it is an eco-friendly approach that involves the use of natural bioresources and avoids toxic chemicals to synthesize different types of NPs. The green method involves using Leek extract, which is a reducing agent and coating for nanoparticles, to study the effect of the preparation of NPs on antibacterial activity utilizing the good diffusion procedure and the physical characterizations of the MnO_2 NPs.

2. Materials and Methods

2.1. Preparation of (leek) leaves extract

10gm of fresh leek leaves were used to produce the leek leaf extract. The leek leaves were properly cleaned using deionized (DI) water to get rid of any dirt and impurities before being dried by air. The dried leaves had been broken up into little bits and put through a mechanical mill after being ground up and placed in a 250ml beaker. The 100ml of DI water was then added, and the mixture was agitated for 60 minutes at 30°C. After cooling to room temperature, the resultant leek leaf extract was filtered. The filtrate was collected and stored at (4°C) in an airtight glass bottle for subsequent use.

2.2. Green Synthesis of (MnO_2) NPs

For the biogenic synthesis of manganese dioxide Np_s the leaves of leek were cut and dried and heated for 60 minutes at 30°C with continuous stirring, then 10 gm of manganous Sulphate monohydrate ($MnSO_4.H_2O$) (10 mM) was added to (100 ml) of leek leaf extract **Figure 1**. The resulting mix was treated with an ultrasonic bath for 10 minutes and then shaken at 30 °C for 24 hours for redox and capping reactions. The samples were centrifuged at 3500 rpm for 10 min. After centrifugation, the MnO_2 NP_s were washed three times with distilled water, dried in an oven, and then calcinated at (200°C) for six hours. Notice that the mixture color changed slowly from greenish to light yellowish, and after drying, the powder became dark brown. The green synthesized MnO_2 NP_s were stored after they were crushed.

Figure 1. Diagrammatic illustration of the synthesis process used to create green MnO_2 NP_s using leek leave extract.

3. Result and dissuasion

3.1. Ultraviolet-visible (UV-Vis) analysis

(UV-Vis) spectroscopy is the most practicable technique for characterizing NP_s. The generation and stability of nanoparticles in an aqueous colloidal solution are supported by (UV-Vis) spectral spectroscopy [13]. The (UV-Vis) absorption spectra of the created MnO_2 NP_s as well as biofunctionalized nanoparticles were measured on a (UV-Vis) spectrophotometer. Figure 2 shows the MnO_2NP_s' UV-Vis spectrum. Generally, color changes seen during the reaction signify the production of NP_s and stability [14]. The color shift from greenish to light yellowish brown is due to the surface plasmon resonance (SPR) band of the synthesized metal nanoparticles, which depend on the size, shape, and distribution, which indicated the stabilization of MnO_2NP_s were indicative of these processes. The unique properties of size, shape, and distribution give metal oxide nanoparticles excellent processability, making them potential candidates for antibacterial applications. [15]. **Figure 2** shows that MnO_2NP_s had two distinct peaks at 257.5 and 290 nm, which appeared as humps. The samples exhibit two distinct absorption peaks at 287.5 and 291 nm, each of which is connected to the MnO_2 NP_s' band gap absorption [15]. The absorption spectra of the MnO_2 NP_s with varied impurities are displayed by the absorbance peaks at 287.5 and 291 nm. The MnO_2 NP_s displayed maximum absorbance at 287.5 nm. The energy band gap (E) of manganese dioxide nanoparticles was calculated using the formula:

$$E= (hc/ \lambda_{max})$$

where h = (6.626×10^{-34} J.s) is planks constant, c = (3×10^{8} m/s) the speed of light, E is the band-gap energy, and λ_{max} is the nanoparticle's wavelength. (UV–vis) The energy band was measured to be (4.31) eV, and the MnO_2 bulk had an energy band of (2.37) eV. The results show that the band gap energy increases with decreasing particle size. Because of the confinement of the electrons and holes, the band gap energy increases between the valence band and the conduction band while decreasing the particle size based on the quantum confinement theory[16].

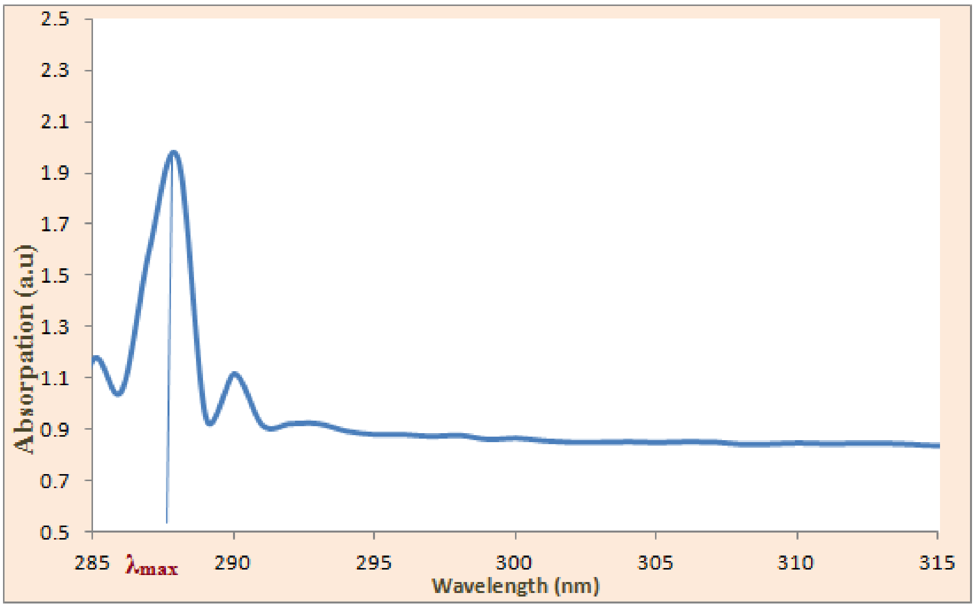

Figure 2. (UV- Vis) specter image of Manganese Dioxide - NP_s .

3.2. XRD analysis

X-Ray Diffraction Using powder (X-ray) diffraction spectroscopy (XRD) at a wavelength of (0.154 nm), the crystalline and phase purity of the green-produced MnO_2 NP_s were identified. The XRD spectra were captured in the range (10°–80°). An X-ray diffractometer using Cu Kα radiation was used [17, 18] . The MnO_2 NPs' XRD pattern figure (3) exhibits a broad pattern that has been linked to the presence of bio-capped as well as amorphous materials; diffraction peaks were observed at 2θ. A known orthorhombic structure in MnO_2 can be correlated with reflection values of 12.94, 18.34,28.78, 37.66, 42.14, 60.26 and73.72 degrees (JCPDS no. 44-0141). MnO_2 NP_s were successfully synthesized, as indicated by the strong XRD peaks [19]. The Debye-Scherrer equation[20],

$$\text{Crystalline size (D)} = k\lambda / \beta \cos \theta \qquad (1)$$

Where k: is the shape factor (0.94), λ: the incident radiation's X-ray wavelength (0.154252) nm,β: (FWHM) is the full-width half maximum, and θ: is the Bragg's angle, which takes into account the (X-ray) wavelength (0.154 nm), the width of a peak with maximum intensity in half height, the crystal's thickness (d), the diffraction angle, and the Debye-Scherrer constant (0.9)[21, 22]. Table 1 shows the crystal size values of Manganese Dioxide NP_s with the highest intensity obtained by the green technique from leek aqueous extracts. The mean crystalline size of Manganese Dioxide NP_s is 34.07 nm.

Table 1. The crystalline sizes(D) of Manganese Dioxide Nanoparticles produced from leek leaves aqueous extract.

2θ (Deg.)	**(FWHM) (Deg.)**	**Crystalline size D(nm)**	**Hkl**
18.34	0.2683	30.07	(200)
28.78	0.2228	36.90	(310)
37.66	0.2976	28.26	(211)

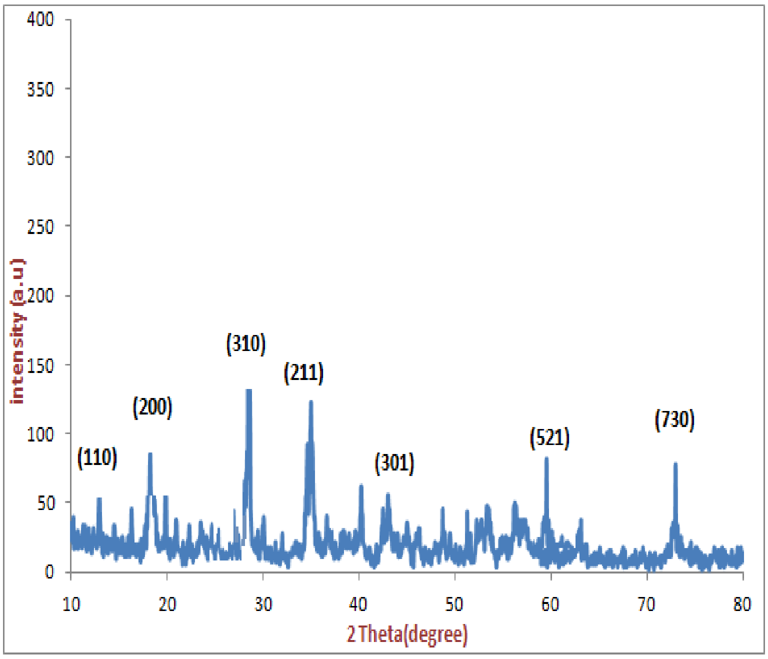

Figure 3. XRD image of MnO_2 – NP_s.

3.3. FE-SEM Field Emission Scanning Electron Microscopy Analysis

Field emission scanning electron microscopy (FESEM) investigates each particle, including the aggregation of particles, and can visualize crystal structure, surface morphology, distributed and aggregated nanoparticles, and surface fictionalization[23, 24]. Rocky spherical MnO_2 NP_s were successfully produced. The rocky spherical MnO_2 NP_s distributed and made with Leek aqueous extract are shown in the (FESEM micrographs in **Figure 3**. The MnO_2 nanoparticles have a stony, compacted shape [23,25]. The photos display the presence of secondary material surrounding the MnO_2, which pointed to the bioorganic components that produced and stabilized the rocky, spherical MnO_2 NP_s [26]. The average nanoparticle grain size was evaluated to be between 29 and 85 nm in size. The size, shape, and aggregation pattern of the nanoparticles depend on the quantity-based presence of phytochemicals in plants. This could be effective in reducing, capping, and stabilizing nanoparticles to narrow sizes with rocky spherical shapes, resulting in highly agglomerated nanoparticles.

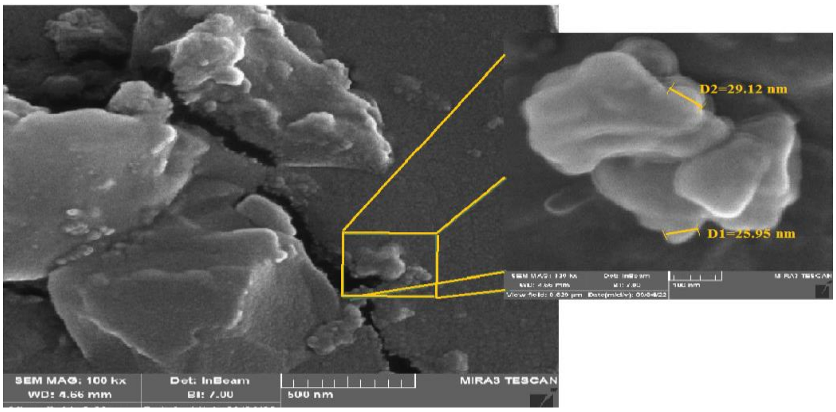

Figure 3. FE-SEM of MnO_2-NP_s.

3.4. Energy Dispersive X-ray (EDX) Analysis

Energy Dispersive X-ray (EDX) analysis of the MnO_2 Np_s is an important tool used to identify the elemental composition of materials. **Figure 4** displays the EDX patterns; the peak values for lines of O were 0.535 and 1.7 keV, and for lines of Mn elements, they were 0.54 and 5.94 keV. According to the strength of the lines, which is shown in **Figure 4**, the percentages of Mn and O were calculated. In the EDX, Mn (21.54%) and O (43%) are shown respectively.

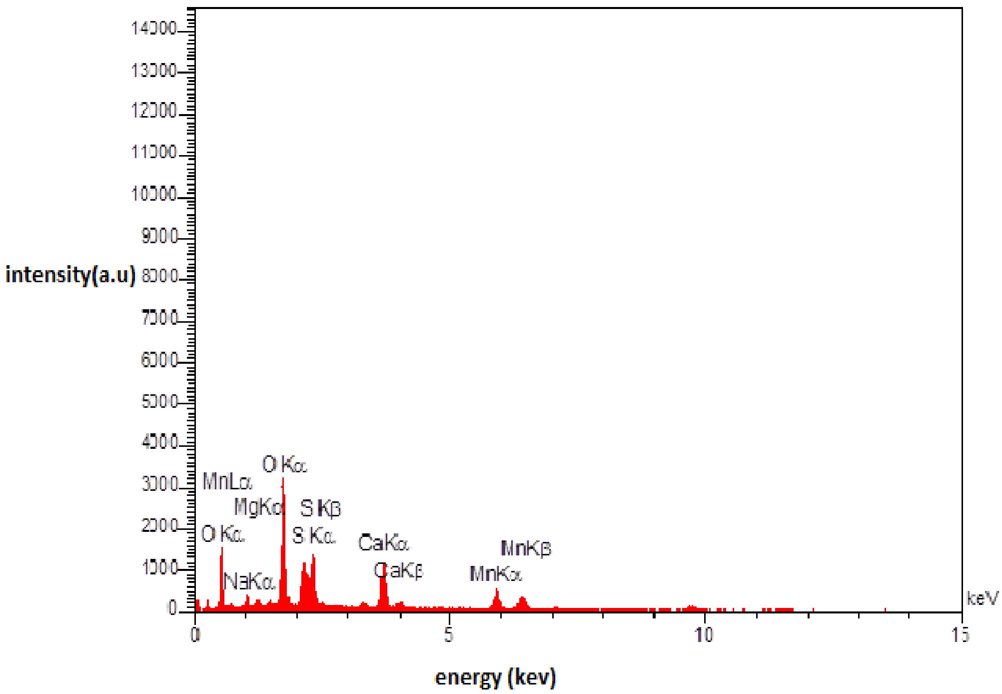

Figure 4. EDX for MnO_2NP_s by green method.

3.5. AFM Analysis

This technique provides an idea of the crystalline nature of the layer, where phase morphology and height images can be recorded. The height image provides terrain information. In addition, the surface roughness can be measured by AFM. The method for preparing an AFM sample with the Manganese dioxide-coated surface facing upward on a thin glass plate was to evenly spread out the sample and allow it to air dry[27, 28]. An atomic force microscope was used to obtain AFM pictures. MnO_2 NPs are visible as agglomerated particles in the AFM picture of MnO_2 (**Figure 5-A**). Most MnO_2 NPs recorded an average diameter of (50.20) nm. In AFM, the surface roughness can be measured in terms of the average diameter roughness; it was 32.94 nm, and AFM images confirm the measured RMS roughness was 40.6 nm. The morphological analysis also showed that the NPs have a spherical form. These AFM pictures demonstrate the significant nanoparticle adsorption on the MnO_2 nanoparticle substrate surface. Analysis of the AFM pictures reveals a rocky-like structure with a limited size distribution (2D and 3D views). The graph of particle size distribution is shown in **Figure (5-C)** as well.

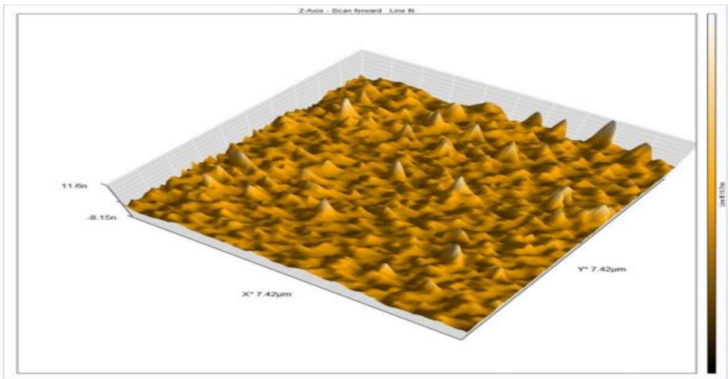

(A)

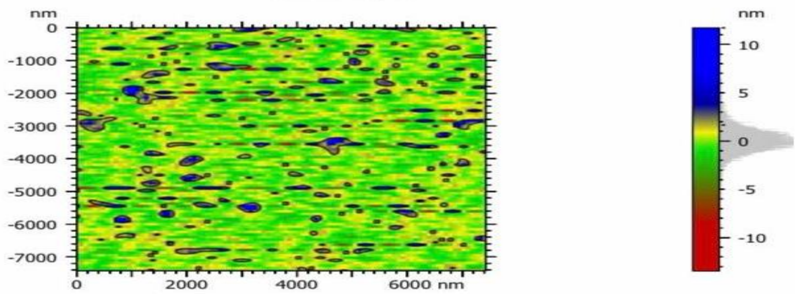

Information		
Method	Threshold detection	
Threshold 1	1.715	nm
Number of particles	50.20	
Coverage	7.028	%
Density	3794184	Particles/mm²

(B)

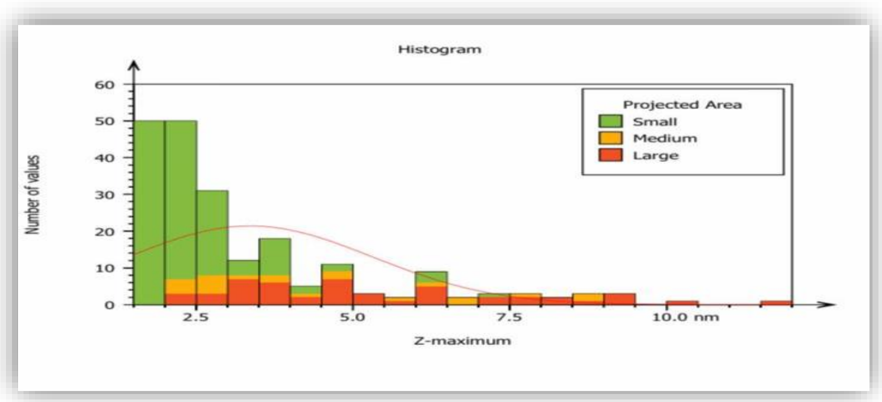

(c)

Figure 5. Represents AFM scans, where (a) is a 3D image, (b) is a 2D image, and (c) represents the distribution of MnO_2- NPs created using the Green technique with leek extract.

3.6. Antibacterial Activity

Antibacterial activity using the well agar approach was assessed, and the antibacterial potency of the produced MnO_2 NP_s was assessed against (Klebsiella, E.coli, and Staphylococcus aureus. Typically, the different bacterial strains were seeded into separate Mueller-Hinton agar plates and then cultivated for 24 hours at 37°C. Their cell density was kept at (1.5 X 108 CFU/ml). (1.5 X 108 CFU/ml) microorganism cells were swabbed onto a plate of Mueller-Hinton agar. The duplicate serial dilution was prepared from the stock solution, which was (1000,500, 250,125,62.5) μg/ml. By placing MnO_2 nanoparticles in the appropriate wells, holes punched in the agar (7-mm-diameter holes) plates were examined to determine the zone of inhibition. They were incubated for 24 hours at 37 °C. If there is a wide, clear zone surrounding the producer strain colonies, the inhibition is considered positive. The wider inhibition zone may be seen around the wells, indicating that MnO_2 Np_s are responsible for the sensitive bacteria's inhibition[29, 30] .Based on how effectively different bacterial strains were killed, the antibacterial activity of MnO_2 NP_s was assessed. The CFU of E. coli, K. pneumoniae, and S. aureus were all reduced in the MnO_2 NP_s synthesized from leek extracts, according to the results. With a zone of inhibition of 33 mm for Staphylococcus aureus.

The MnO_2 NPs showed better performance of antibacterial activity for S. aureus compared with k. pneumoniae and E. coli bacterial strains, which had zones of inhibition of 30 and 25 mm for(klebsiella pneumonia) and (Escherichia coli), respectively as shown in **Figure 6.** It is concluded from the previous results that plant extracts can produce MnO_2 NP_s, with antibacterial activity. The MnO_2 NP_s showed better antibacterial activity and were more efficient against gram-positive bacteria than gram-negative bacteria[12]. The experimental results demonstrate that MnO_2 NPs are effective antibacterial agents. The antibacterial activity of MnO_2 NPs is related to their small size; they can easily enter bacterial cells and damage cell membranes. Finally, it results in bacterial cell death as a result of bacterial cell deformation processes. Here, we mostly display the outcomes of them in **Table 2**.

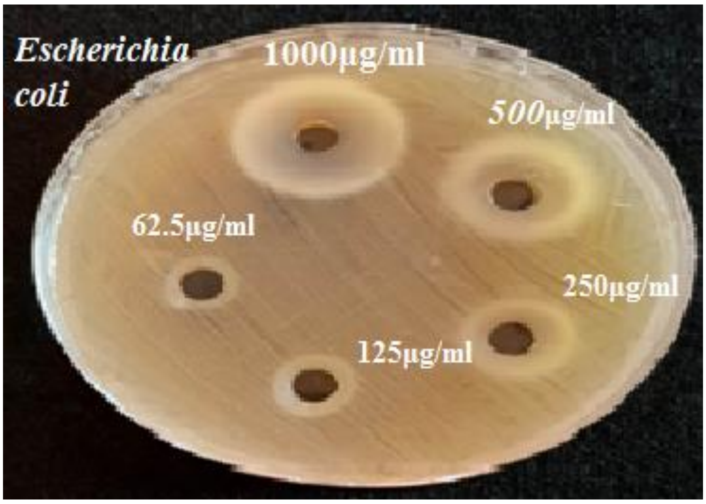

(a)

a 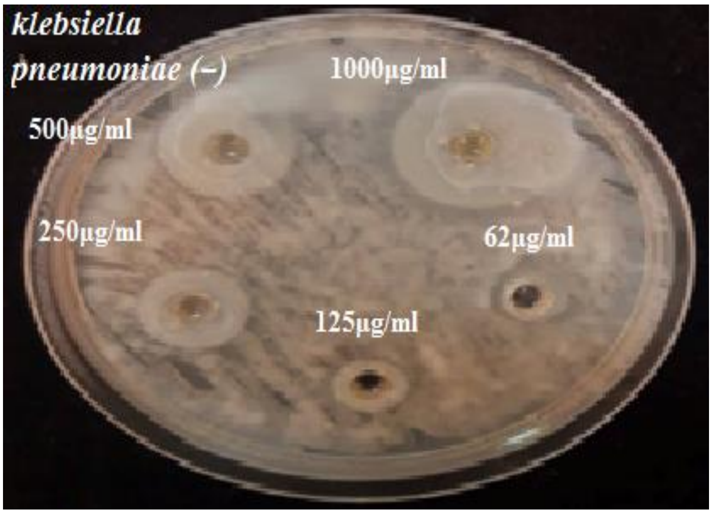

(b)

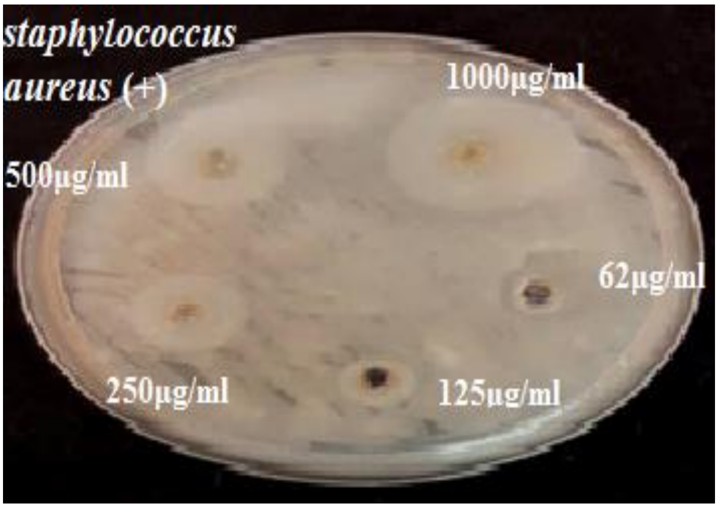

(c)

Figure 6. The antimicrobial activity of MnO_2 –NPs.

Table 2. Antibacterial activity of Manganese Dioxide Nanoparticles

Microorganisms	**Zone of inhibition (mm)**				
	(1000) µg/ml	**(500) µg/ml**	**(250) µg/ml**	**(125) µg/ml**	**(62.5) µg/ml**
E. coli (−)	25	22	17	9	5
k. pneumoniae (−)	30	23	18	12	6
S. aureus (+)	33	26	19	12	6

Antibacterial activity at the same concentration was also detected **Figure 7**. Similarly, MnO_2-Np_s inhibits S. aureus the most. MnO_2-Np_s has shown good inhibition for S. aureus and lower efficient antibacterial activity against the bacterial k. pneumonia and E. coli due to its sensitivity to bacterial strains.

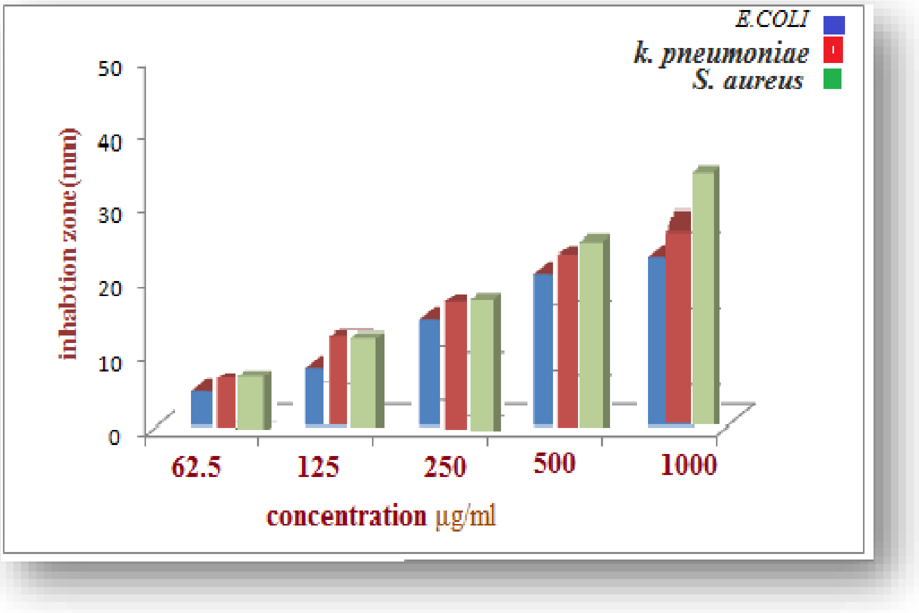

Figure 7. The antibacterial activity assay with the inhibition zone and the concentration of MnO_2-NP$_s$ against E. coli, k. pneumoniae , S. aureus.

4. Conclusion

Manganese Dioxide nanoparticles were synthesized by the green synthesis method using manganous sulfate monohydrate ($MnSO_4.H_2O$). The obtained MnO_2 was characterized by a (UV-vis) study that confirmed the visible color change from green to dark brown, which resulted in the synthesis of MnO_2 NPs. The development of orthorhombic structures in the XRD investigation revealed the crystallinity of MnO_2 NPs. The morphological analysis of the synthesized MnO_2 NPs using FESEM indicated that the nanoparticles were spherical, with average grain sizes estimated to be between 30 and 85 nm in size. Thus, MnO_2 nanoparticles are used in green synthesis. The development of nanotechnology has recently placed a strong emphasis on procedures that make use of mild reaction conditions and nontoxic precursors. The formulated MnO_2-Nps inhibited the growth of S. aureus, K. pneumoniae, and E. coli, with a higher activity at concentrations (1000µg/ml).

Acknowledgments

I extend my thanks to the Department of Physics, College of Sciences for Women, University of Baghdad for assisting in completing this work by opening private laboratories and providing scientific facilities by the staff of the Physics Department to help support the research project.

Conflict of interest

The authors declare that they have no conflict of interest.

Funding

None.

References

1. Patil, S., Sivaraj, R., Rajiv, P., Venckatesh, R. and Seenivasan, R.Green synthesis of silver nanoparticle from leaf extract of Aegle Marmelos and evaluation of its antibacterial activity. *Int J Pharm Pharm Sci*

2015, *7*(*6*), 169-173.
2. Shanan, Z.J.; Hadi, S.M.; Shanshool, S.K. Structural analysis of chemical and green synthesis of CuO nanoparticles and their effect on biofilm formation. *Baghdad Science Journal* **2018**, *15*(*2*), 211-221. http://dx.doi.org/10.21123/bsj.2018.15.2.0211.
3. Treutter, D. Significance of flavonoids in plant resistance: a review. *Environmental Chemistry Letters* **2006**, *4*(*3*), 147-157. https://doi.org/10.1055/s-2005-873009.
4. Abdulameer, S.A.; Kadhim, R.E. Green Synthesis of Manganese Oxide Nanoparticles by Aqueous Extract of Conocarpus Erectus L. Leaves. *HIV Nursing* **2023**, *23*(*3*), 20-29. https://doi.org/10.1016/j.matpr.2022.03.563.
5. Ramanujam, K.; Sundrarajan, M. Antibacterial effects of biosynthesized MgO nanoparticles using ethanolic fruit extract of Emblica officinalis. *Journal of photochemistry and photobiology B: biology* **2014,** *141*(*4*), 296-300. https://doi.org/10.1016/j.jphotobiol.2014.09.011.
6. Kumari, P.; Kureshi, A.A. Green Synthesis of Photocatalysts and its Applications in Wastewater Treatment. Photoreactors in Advanced Oxidation Processes. *The Future of Wastewater Treatment*, **2023,** *23*(*4*), 71-108. http://dx.doi.org/10.9790/264X-0403017883.
7. Srinivasan, K. Black pepper and its pungent principle-piperine: a review of diverse physiological effects. *Critical reviews in food science and nutrition* **2007**, *47*(*8*), 735-748.
8. Periakaruppan, R.; Naveen, V.; Danaraj, J. Green synthesis of magnesium oxide nanoparticles with antioxidant potential using the leaf extract of piper Nigrum. *JOM.* **2022**, *74* (*12*), 4817-4822. https://doi.org/10.1016/j.inoche.2022.110156.
9. Sellami, H. Olea europaea mediated bioengineered biocompatible gold nanoparticles for antimicrobial, cytotoxic applications, and molecular docking study. *Journal of King Saud University-Science* **2022**, *34*(*6*), 102133. https://doi.org/10.1007/s10098-022-02329-7.
10. Varma, P.K. Endophytes: role and functions in crop health. *Plant-Microbe Interactions in Agro-Ecological Perspectives* **2017**, *23*(*4*), 291-310. https://doi.org/10.1016/B978-0-444-64325-4.00005-5.
11. Fornes, O. JASPAR 2020: update of the open-access database of transcription factor binding profiles. *Nucleic acids research* **2020**, *48*(*1*), 87-92. https://doi.org/10.1093/nar%2Fgkx1188.
12. Lu, H. Biogenic synthesis of MnO2 nanoparticles with leaf extract of Viola betonicifolia for enhanced antioxidant, antimicrobial, cytotoxic, and biocompatible applications. *Frontiers in Microbiology* **2021**, *12*(*5*), 761084. https://doi.org/10.1016/j.rechem.2023.101266.
13. Sasani, G.M. Impact of nanostructured thin ZnO film in ultraviolet protection. *International journal of nanomedicine* **2017**, *12*(*2*), 207-216. http://dx.doi.org/10.2147/IJN.S118637.
14. Jayandran, M.; Haneefa, M.M.; Balasubramanian, V. Green synthesis and characterization of Manganese nanoparticles using natural plant extracts and its evaluation of antimicrobial activity. *Journal of Applied Pharmaceutical Science* **2015**, *5*(*12*),105-110. https://doi.org/10.17485/IJST%2F2016%2FV9I3%2F80523.
15. Souri, M. Procedure optimization for green synthesis of manganese dioxide nanoparticles by Yucca gloriosa leaf extract. *International Nano Letters* **2019**, *9*(*2*), 73-81. https://doi.org/10.1007/s40089-018-0257-z.
16. Rosetti, R., Excited electronic states and optical spectra of ZnS and CdS crystallites in the≅ 15 to 50 Å size range: evolution from molecular to bulk semiconducting properties. *J. Chem. Phys.* **1985,** *82*(*3*), 552-559. https://doi.org/10.1016/j.saa.2020.119369.
17. Yallappa, S. Microwave-assisted rapid synthesis and biological evaluation of stable copper nanoparticles using T. arjuna bark extract. *Spectrochimica Acta Part A: Molecular and Biomolecular Spectroscopy* **2013**, *110*(*2*), 108-115. https://doi.org/10.1016/J.MOLSTRUC.2018.05.004.
18. Naidja, A. Synthesis and characterization of cryptomelane (α-MnO2) nanoparticles: Influence of phthalic acid adsorption and oxidation on the mineral structure. *Inorganic and Nano-Metal Chemistry* **2022**, *52*(*1*), 42-52. https://doi.org/10.1080/24701556.2020.1862220.
19. Christensen, L. Biosynthesis of silver nanoparticles using Murraya Koenigii (curry leaf): an investigation on the effect of broth concentration in reduction mechanism and particle size. *Advanced*

Materials Letters **2011**, *2*(*6*), 429-434. https://doi.org/10.13074/jent.2020.06.203415.

20. Ali, M. Structural and optical properties of upconversion CuInS/ZnS quantum dots. *Optical Materials* **2018,** *86*(*3*), 545-549. https://doi.org/10.3390%2Fnano12193470.
21. Gao, L.J. Grain-controlled barium titanate ceramics prepared from high-gravity reactive precipitation process powder. *Materials chemistry and physics* **2004,** *88*(*1*), 27-31. https://doi.org/10.1016/J.MATCHEMPHYS.2004.03.023.
22. Shanan, Z.J.; Abdalameer, N.K.; Ali, H.M. Zinc Oxide Nanoparticle Properties and Antimicrobial Activity. *International Journal of Nanoscience* **2022**, *21*(*3*), 2250017. http://dx.doi.org/10.5923/j.nn.20150501.01.
23. Hoseinpour, V. Surface modification of PES membrane via aminolysis and immobilization of carboxymethylcellulose and sulfated carboxymethylcellulose for hemodialysis. *Carbohydrate polymers* **2018**, *188*(*4*), 37-47. https://doi.org/10.1016/j.carbpol.2018.01.106.
24. Ali, R. Green synthesis and the study of some physical properties of MgO nanoparticles and their antibacterial activity. *Iraqi Journal of Science* **2020**, *23*(*4*), 266-276. https://doi.org/10.24996/ijs.2020.61.2.9.
25. Jayaseelan, C. Novel microbial route to synthesize ZnO nanoparticles using Aeromonas hydrophila and their activity against pathogenic bacteria and fungi. *Spectrochimica Acta Part A: Molecular and Biomolecular Spectroscopy* **2012,** *90*(*3*), 78-84. https://doi.org/10.1016/j.saa.2012.01.006.
26. Vickers, N.J. Animal communication: when I'm calling you, will you answer too. *Current biology* **2017,** *27*(*14*), 713-715. https://doi.org/10.1016/j.cub.2017.05.064.
27. Corneal, L.M. AFM, SEM and EDS characterization of manganese oxide coated ceramic water filtration membranes. *Journal of Membrane Science* **2010**, *360*(*2*), 292-302. https://doi.org/10.1016/j.memsci.2010.05.026.
28. Sinha, A. Synthesis and characterization of monodispersed orthorhombic manganese oxide nanoparticles produced by Bacillus sp. cells simultaneous to its bioremediation. *Journal of Hazardous Materials* **2011**, *192*(*2*), 620-627. https://doi.org/10.1016/J.CPLETT.2004.11.028.
29. Abuzeid, H. Green Synthesized α-MnO 2 As a Photocatalytic Reagent for Methylene Blue and Congo Red Degradation. *Journal of Electronic Materials* **2021**, *50*(*2*), 2171-2181.
30. 30.Mohr, K.I. History of antibiotics research. How to Overcome the Antibiotic Crisis: Facts, Challenges. *Technologies and Future Perspectives* **2016,** *23*(*4*), 237-272. https://doi.org/10.1007/82_2016_499.